analytical chemistry

Technical Note

pubs.acs.org/ac

Eco-Friendly Plasmonic Sensors: Using the Photothermal Effect to Prepare Metal Nanoparticle-Containing Test Papers for Highly Sensitive Colorimetric Detection

Shao-Chin Tseng,[†] Chen-Chieh Yu,[†] Dehui Wan,[†] Hsuen-Li Chen,*[,†] Lon Alex Wang,[‡] Ming-Chung Wu,[†] Wei-Fang Su,[†] Hsieh-Cheng Han,[§] and Li-Chyong Chen[§]

[†]Department of Materials Science and Engineering, National Taiwan University, Taipei, Taiwan

[‡]Graduate Institute of Photonics and Optoelectronics, National Taiwan University, Taipei, Taiwan

[§]Center for Condensed Matter Science, National Taiwan University, Taipei, Taiwan

Supporting Information

ABSTRACT: Convenient, rapid, and accurate detection of chemical and biomolecules would be a great benefit to medical, pharmaceutical, and environmental sciences. Many chemical and biosensors based on metal nanoparticles (NPs) have been developed. However, as a result of the inconvenience and complexity of most of the current preparation techniques, surface plasmon-based test papers are not as common as, for example, litmus paper, which finds daily use. In this paper, we propose a convenient and practical technique, based on the photothermal effect, to fabricate the plasmonic test paper. This technique is superior to other reported methods for its rapid fabrication time (a few seconds), large-area throughput, selectivity in the positioning of the NPs, and the capability of preparing NP arrays in high density on various paper substrates. In addition to their low cost, portability, flexibility, and biodegradability, plasmonic test paper can be burned after detecting contagious biomolecules, making them safe and eco-friendly.

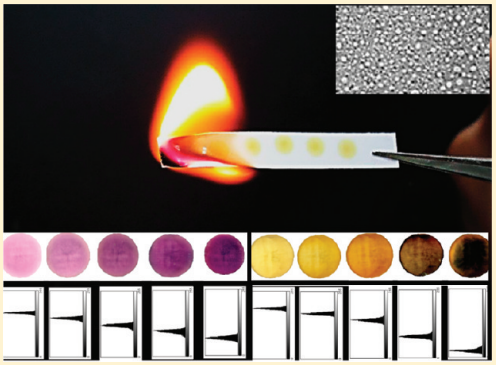

Paper has been developed and used as a supporting material for over 1000 years. It provides flexibility, thinness, a low volume, wide accessibility, lightweight, and abundant storage capability, in addition to being much cheaper than other substrates. For example, the price of paper is approximately 0.1 cent dm^{-2}, whereas the plastic substrates polyethylene terephthalate (PET) and polyimide (PI) cost approximately 2 and 30 cent dm^{-2}, respectively.[1] Furthermore, the rate of paper manufacturing through roll-to-roll (R2R) processing usually exceeds 100 km h^{-1}.[1]

Paper substrates have been developed for electronic devices, digital displays,[2] and photovoltaic devices.[3] Because paper substrates are compatible with printing processes (e.g., screen printing, inkjet printing, flexo printing), the fabrication of paper-based devices can be much faster and simpler than the use of traditional semiconductor processing. Another common use of paper substrates is the preparation of test paper or indicator paper; for example, gas,[4] pH,[5] and temperature sensors[6] have all been established on paper substrates. Paper-based biosensors are also very attractive because they are cheap, burnable, biodegradable, and thus eco-friendly.[7−10]

Biosensing techniques based on spectroscopic analysis, colorimetric detection, and surface-enhanced Raman scattering (SERS) have been studied widely.[11−17] Enhancing the electric field around the probe can improve the signal intensity dramatically, thereby increasing the sensitivity and potentially allowing extremely small amounts of analytes to be detected. Metal nanoparticles (NPs) have been applied widely in biosensors because unique localized surface plasmon resonance (LSPR) phenomena lead to strong electric field intensities around the NPs. The strong electric field enhancement around the particles makes NP-based biosensing extremely sensitive; therefore, only small amounts of analytes are required for testing.

To prepare NPs on paper substrates, the most common method is the drying of a colloidal solution of NPs on a paper substrate. The Zhao group coated DNA-cross-linked Au NP aggregates onto paper substrates.[18] The chemically synthesized Au NPs dried directly and aggregated on paper substrates that had been treated hydrophobically. These Au NP assays on paper substrates were used as colorimetric probes. However, the need for repeated drying of the paper makes this method complicated. Moreover, Yu et al. used an inkjet printing method to prepare metal NP arrays on a cellulose paper substrate.[19] They synthesized NPs in a colloidal solution, using the conventional method reported by Lee and Meisel[20] and then printed them onto a paper substrate using an inkjet printer. It is, however, difficult to obtain highly dense NP arrays

Received: December 8, 2011
Accepted: April 30, 2012
Published: April 30, 2012

   dx.doi.org/10.1021/ac300397h | *Anal. Chem.* 2012, 84, 5140−5145

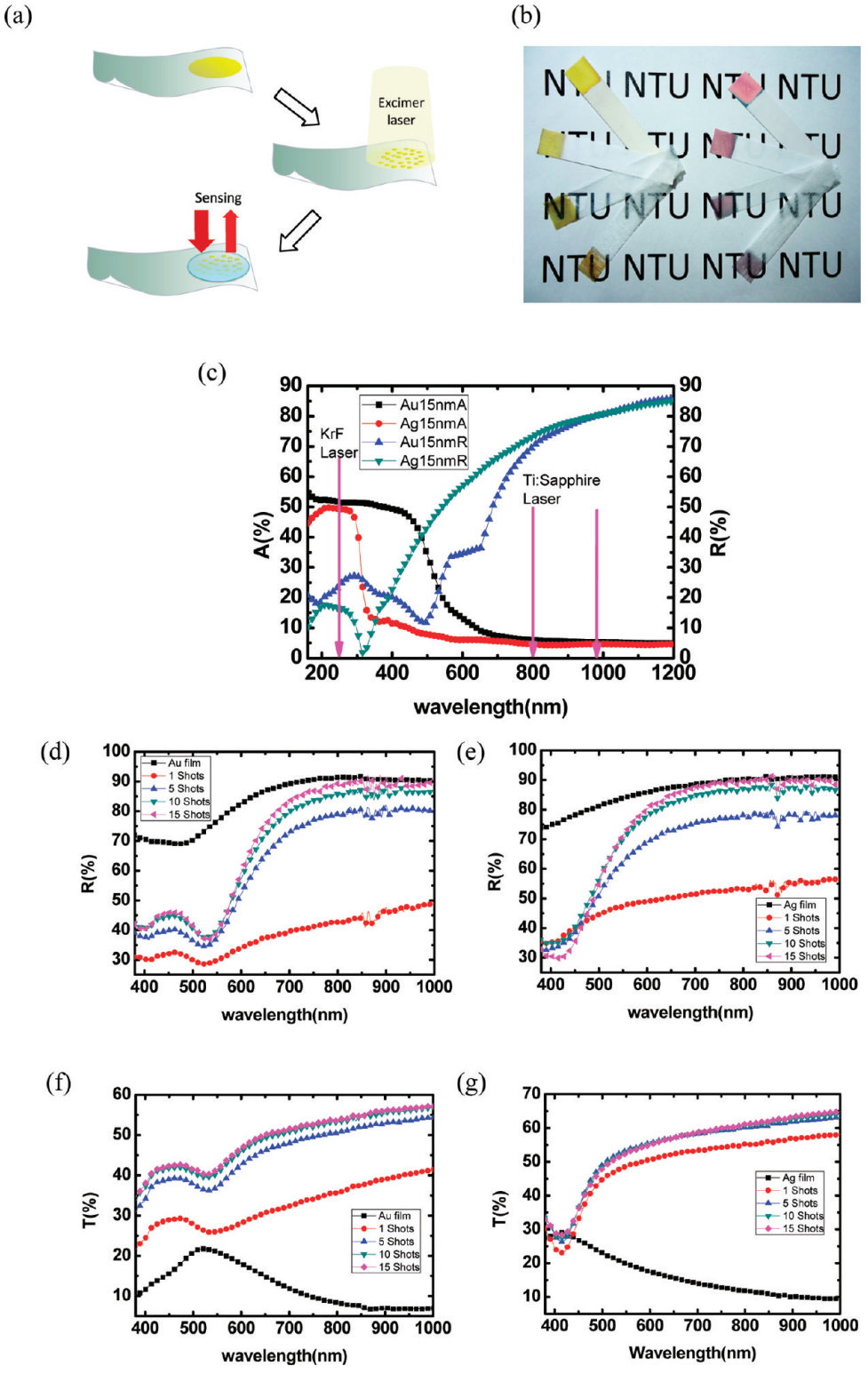

Figure 1. (a) Schematic representation of the preparation of the NP-containing test paper. (b) Photographic images of Ag (left) and Au (right) NP-containing test papers prepared from photographic paper, inkjet printing paper, waxed paper, and nonwoven fiber sheets (from top to bottom). (c) Absorbance and reflectance spectra of Au and Ag films having a thickness of 15 nm. (d, e) Reflectance spectra of (d) Au NP- and (e) Ag NP-containing test papers prepared from photographic paper and (f, g) transmission spectra of (f) Au NP- and (g) Ag NP-containing test papers prepared from waxed paper, with different numbers of shots of laser irradiation.

when using this method. Low-density NP arrays result in much weaker LSPR-induced absorption, making it difficult to observe signal changes through colorimetric measurement. He et al. have formed noble metal NPs, including Au, Ag, Pd, and Pt NPs, in situ on cellulose paper substrates by immersing the paper sheets into solutions containing metal ion precursors and reducing agents.[21] Ultrasound-assisted preparation methods have also been proposed. Gottesmanet et al. immersed paper

dx.doi.org/10.1021/ac300397h | *Anal. Chem.* 2012, 84, 5140−5145

substrates into silver precursor solutions, together with ultrasonic radiation, to form Ag NPs on the substrate.[22] Generally, the procedures reported for depositing chemically synthesized NPs or forming them on paper substrates are either complicated solution processes or result in low densities of NPs on the paper; therefore, there remains much room for improvement.

Because paper based substrates perform poor wettability,[23,24] methods based on physical formation are more appropriate when fabricating NP-containing paper substrates. Physical formation methods are generally based on electron beam or focused ion beam lithography. Although lithographic methods can be used to precisely define the morphologies and sizes of NPs, the high cost of these complicated processes decreases their practicality for the large-scale production of NP-based biosensors. Thermal annealing treatment of thin metal films can also be used to form metal NPs. The major limitation of thermal processing, however, is that the annealing treatment affects both the thin metal film and the underlying substrate. An alternative method is laser-induced annealing, based on the photothermal effect. When laser light is applied, a metal film will absorb the photon energy and transform it into thermal energy. Only the area that is illuminated by the laser gets heated; therefore, localized formation of NPs is readily achieved by controlling the laser spot size and position. Therefore, this method has the ability to create multiple NP-based sensing chips on one single test paper, broadening the varieties of analytes that could be detected by just one test paper. Laser-induced annealing is a potentially rapid and simple method for fabricating disposable biosensors at low cost.[25]

Therefore, we proposed a new technique for fabricating NP-containing test papers based on the laser-induced annealing method. Also the as-fabricated NP-containing test papers could be developed into simple, inexpensive, easy-to-use, portable, disposable, eco-friendly, and highly sensitive LSPR-based biosensors and thus could improve the health care in the developed world and impoverished areas.

EXPERIMENTAL SECTION

Preparing of NP-Containing Test Papers. The 15 nm-thick thin metal films (Au, Ag) were deposited on paper-based substrates through a sputter system; the samples were further irradiated with a KrF excimer laser (Lambda Physik, Compex 150T, 248 nm) having a pulse width of 20 ns and a power density of 65 mJ/cm^2. The illumination spot size was 2 cm^2.

Characterization. The optical spectra of test papers were measured by an optical spectrometer (Hitachi, U4100). The morphologies of the samples were observed using a JEOL JSM-6700F field emission scanning electron microscope. The optical images of the paper samples were scanned using an Epson Perfection V10 home-use scanner. The values of the gray levels were analyzed using Image J, a freely downloadable image analysis software.

RESULTS AND DISCUSSION

Figure 1a presents a schematic representation of the procedure we used to prepare NP-containing test papers. In the first step, we used a sputter system to deposit a thin metal film onto a paper substrate. We then applied the laser-induced photothermal effect to produce metal NPs. Excimer laser light was illuminated on the thin metal film to increase the thermal energy of the metal film, and the metal film was then liquefied. After liquefied, in order to decrease the surface energy, the surface tension made the metal droplets to deform into spherical-like during cooling, leading to the forming of nanoparticles.[26−28] The average diameter of the obtained NPs was determined by the thickness of the deposited thin film and by the laser illumination conditions. Using this approach, we obtained NP-containing test papers. Figure 1b displays photographs of NP-containing test papers fabricated on photographic paper, inkjet printing paper, waxed paper, and nonwoven fiber sheets. The Au NP-containing test papers displayed a clear pink color; the Ag NP-containing test papers were bright yellow. Besides, when using the laser-induced photothermal effect to prepare metal NPs on paper, the wavelength of the laser source must be coincident with the spectrum regime of the metal film to ensure a good photothermal conversion efficiency; that is, large absorbance and small reflectance of incident light is desired. If the incident wavelength is mismatched with the absorbance regime of the thin metal film, then the input power of the incident laser must be increased to produce sufficient thermal energy on the metal film. Figure 1c displays the measured absorbance and reflectance spectra of thin Au and Ag films having a thickness of 15 nm. The Au film possessed an absorbance close to 50% at wavelengths of less than 450 nm; the Ag film exhibited high absorbance (∼50%) at wavelengths of less than 300 nm. Notably, a Ti:Sapphire laser (wavelength, 800 nm or 980 nm) has been used previously for metal annealing in the preparation of metal NPs.[29,30] Metal films with high reflectance in the visible and near-infrared (NIR) regimes will require high input power when using visible or NIR regime laser sources to prepare metal NPs. In this study, we applied a KrF excimer laser to efficiently prepare metal NPs on paper substrates through photothermal effects in the deep-UV regime. To prepare the test papers, we first examined the optical characteristics of various paper substrates. We compared four kinds of usual paper substrates: photographic paper, inkjet printing paper, waxed paper, and nonwoven fiber sheets. The detailed discussion of the optical spectra and optical microscopy images of these four paper substrate were provided in the Supporting Information, Figure S1. Because of the optical behaviors, we named photographic paper and inkjet printing paper substrates "reflection-type" test papers, the waxed paper and nonwoven paper substrates were named "transmission-type" test papers. Using the laser-induced photothermal effect to prepare NPs on paper substrates has the advantage that the distribution of NPs can be controlled by varying both the power density and the number of laser pulses. At a fixed laser power, we simply controlled the density of the metal NPs by controlling the number of laser shots. Parts d and e of Figure 1 display reflectance spectra of the Au and Ag NPs immobilized on the photographic paper, respectively. After laser illumination, the metal NPs began to form on the paper substrate. After one shot, there was a relatively low reflectance (∼50%) over the spectral regime. Upon increasing the number of shots of laser irradiation, an obvious LSPR-induced extinctions at 530 (Figure 1d) and 400 (Figure 1e) nm were observed for the Au and Ag NPs, respectively. Parts f and g of Figure 1 present transmittance spectra of the Au and Ag NP-containing waxed paper samples, respectively. The intrinsic transmittance band was due to the interband transitions of the thin metal films. After laser illumination, the NPs began to form, causing LSPR-induced extinction at wavelengths of 530 and 400 nm for the Au and Ag NP-containing test papers,

dx.doi.org/10.1021/ac300397h | Anal. Chem. 2012, 84, 5140−5145

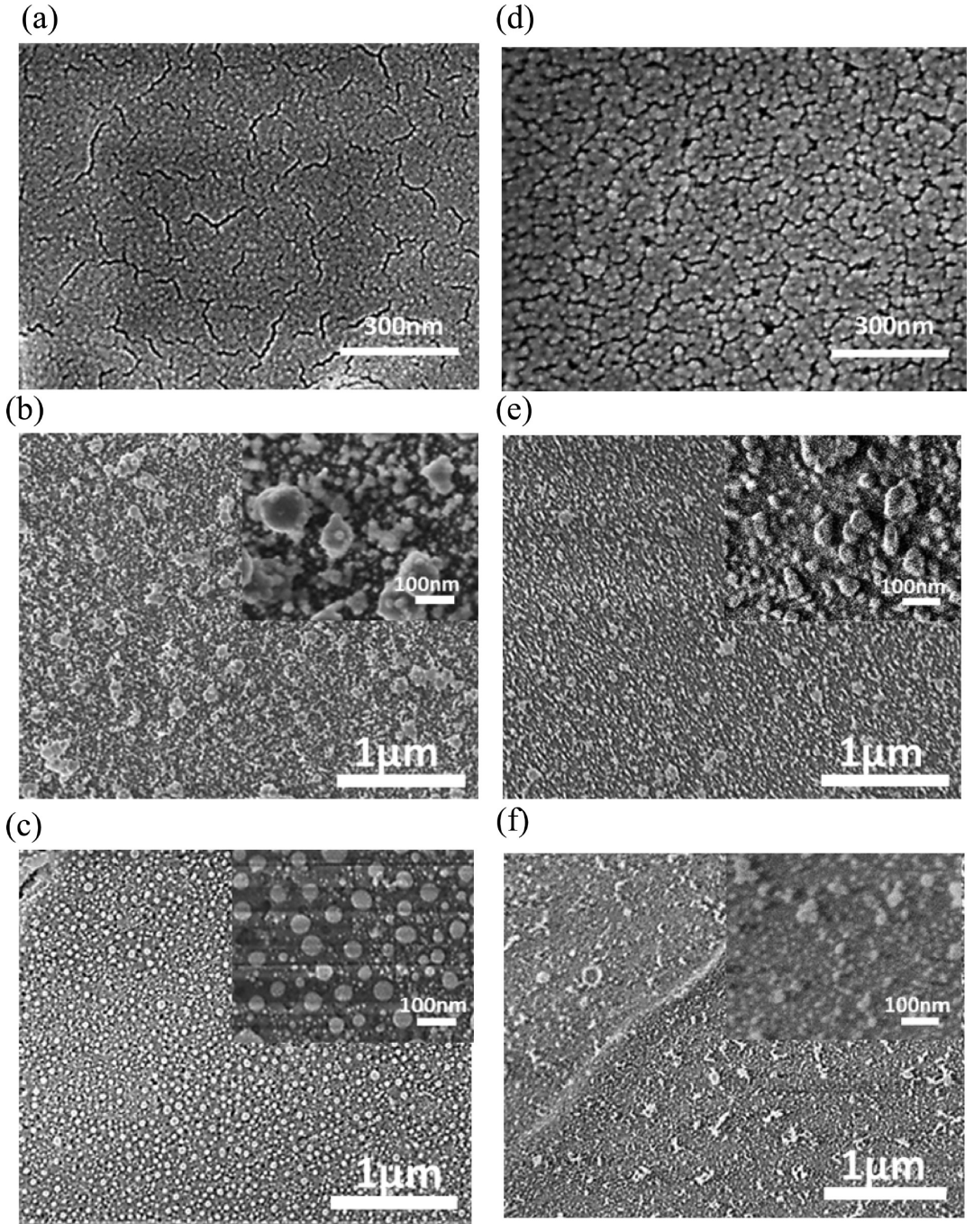

Figure 2. Scanning electron microscopy images of Au NP-containing test papers prepared from (a–c) photographic paper and (d–f) inkjet-printing paper (a, d) before laser illumination and (b, c, e, f) after (b, e) 1 and (c, f) 10 shots. Insets: magnified SEM images.

respectively. In addition, the transmittance increased in the entire spectral regime, except for the wavelength regime of the LSPR, upon increasing the number of shots. From the optical spectra in Figure 1d–g, the reflection-type test papers provided larger signal contrasts than did the transmission-type test papers. We define the signal contrast as the difference in spectral intensity between the nanoparticle-containing test paper in the LSPR wavelength and bulk paper substrate in the same wavelength. For the reflection-type test papers, using the Au NP-containing test paper based on photographic paper (10 shots), as an example, the reflectance difference between the nanoparticle-containing test paper in LSPR wavelength regime (λ = 530 nm) and bulk paper substrate at 530 nm was approximately 58%. In contrast, for the transmission-type test papers, the Au NP-containing test paper based on waxed paper (10 shots), for example, had a relatively low contrast of approximately 29%. Therefore, we suggest that reflection-type test paper might be a better choice for sensor applications. The detailed discussions of the corresponding photographic images of Au NP- and Ag NP-containing test papers prepared from photographic paper, inkjet printing paper, waxed paper, and nonwoven fiber sheets, with different numbers of pulses of KrF laser irradiation are provided in Figure S2 of the Supporting Information.

Next, we used scanning electron microscopy (SEM) to investigate the surface morphologies of the test papers to verify

dx.doi.org/10.1021/ac300397h | *Anal. Chem.* 2012, 84, 5140–5145

the results obtained from the optical spectra. Figure 2a reveals a continuous Au film, as deposited, on the photographic paper. After one shot of laser irradiation, the Au film absorbed the photonic energy to form many island films (Figure 2b). After increasing the number of laser irradiation pulses to 10, the Au film was almost completely transformed into Au NPs (Figure 2c), which were uniform across the entire substrate with an average diameter of 46.31 nm with standard deviation 12.78 nm (measured from the SEM image). Figure 2d displays an SEM image of the Au film deposited on the inkjet printing paper. Compared to the film deposited on the photographic paper, this film possessed a greater roughness that originated from the underlying paper substrate. Figure 2e,f reveals the morphology of the Au film after 1 and 10 shots of laser irradiation, respectively. After one shot of laser irradiation, the Au film on the inkjet printing paper had transformed into some island films. After 10 pulses of laser irradiation, the shapes and diameters (average diameter of 29.91 nm with standard deviation 16.17 nm) of the NPs formed on inkjet printing paper (Figure 2f) were not as uniform as those on the photographic paper (Figure 2c). The variations in the shapes and diameters of these NPs were due to the roughness of the inkjet printing paper influencing the uniformity of the thickness of the as-deposited film. In addition, the rough paper substrate also affected the distribution of the laser energy, leading to uneven formation of NPs. The Ag NP-containing test papers featured morphologies (not shown here) similar to those of the Au NP-containing test papers. Thus, the surface roughness of the paper substrate and the number of shots of laser illumination both had great effects on the structures of the metal NP-containing test papers. The densities of nanoparticles as a function of laser shots were provided in the Supporting Information, Table S1. To be short, the density of nanoparticles would be saturated at 318/μm^2 after 10 shots of laser illumination.

In the last, it is worth mentioning that laser formation method has the advantage of selectivity in the positioning of NPs. Figure 3a,b displays the photograph and optical microscopy images of patterned NP arrays with specific features. We could design the NPs arrays into arbitrary features (Figure 3a) or into square arrays (Figure 3b). The inset SEM image shows the distribution of NPs in each square array. Therefore, this method has the potential to create multiple sensing chips in one single test paper, broadening the varieties of analytes that could be detected by just one test paper. The biosensors described herein, based on metal NP-containing test papers, have the advantage of allowing rapid colorimetric detection, with the color of the test papers changing after the binding of the biomolecules. Much biomedical research[31,32] is focused on the detection of thiol-containing amino acids, particularly cysteine (Cys) and homocysteine, because they play various roles in, for example, acquired immune deficiency syndrome (AIDS) and cardiovascular diseases. Detection of these thiol-containing amino acids is an important aspect of both medical and pharmaceutical science.[31,32] Thus we used our test papers to detect Cys as a demonstration. Figure 4a presents a photographic image of an as-fabricated Ag NP-containing test paper before and after its binding with the Cys targets; the obvious change in color of the test paper reveals the potential for rapid colorimetric detection. Beside the colorimetric detection by naked eyes, spectroscopic detection and gray level detection could utilize the NP-containing test papers as well. A detail discussion of spectroscopic and gray level detection using NP-containing test papers is provided in the Supporting Information (Figure S3). Because biosensors are often applied to the detection of contagious biomolecules, viruses, and bacteria, it is preferable for these analytes to be destroyed immediately after sensing. Paper-based biosensors can be burned after detection of the analytes (Figure 4b), whereas other kinds of substrates (e.g., plastic, glass, semiconductors) cannot. Therefore, paper-based biosensors are considerably safer and more eco-friendly.

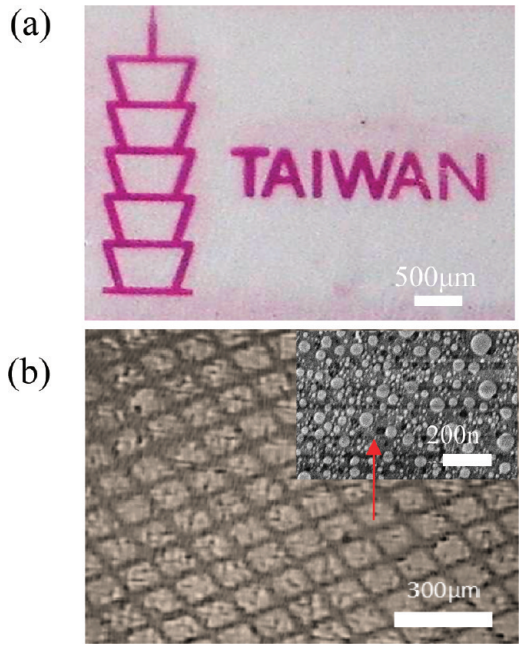

Figure 3. (a, b) Photograph and optical microscopy images of a patterned NP-containing test paper; a design figure (a) and 120 μm square arrays (b) pattern were easily formed by this method. The inset shows the SEM images of the nanoparticles distribution in each square array.

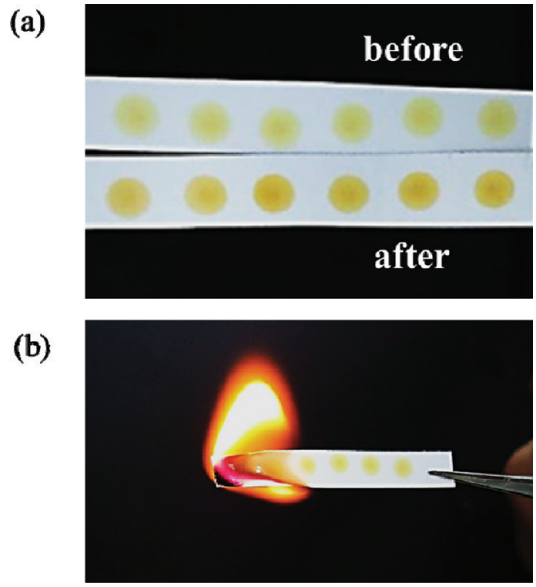

Figure 4. Photographs of the Ag NP-containing test papers (a) before and after binding of 10^{-3} M Cys targets and (b) being burned after sensing to avoid the spreading of contagious biomolecules.

dx.doi.org/10.1021/ac300397h | *Anal. Chem.* 2012, 84, 5140−5145

CONCLUSIONS

We employed the laser-induced photothermal effect to rapidly prepare metal NPs on various paper substrates. Relative to other reported methods, this approach has the advantages of rapid fabrication (requiring only a few seconds), large-area throughput, selectivity in the positioning of the NPs, and the capability of creating NP arrays in high density on paper substrates. We took advantage of the LSPR of metal NPs to enable the fast colorimetric detection of biomolecules. By simply immersing the NP-containing test papers into cysteine solution, the color of the test papers changed and was easily observed by naked eyes. In addition to their portability, flexibility, and biodegradability, biosensors based on paper substrates can be burned after the detection of contagious biomolecules, viruses, and bacteria, making paper-based plasmonic biosensors innately safe and eco-friendly.

ASSOCIATED CONTENT

Supporting Information

Additional information as noted in text. This material is available free of charge via the Internet at http://pubs.acs.org.

AUTHOR INFORMATION

Corresponding Author

*E-mail: hsuenlichen@ntu.edu.tw.

Notes

The authors declare no competing financial interest.

ACKNOWLEDGMENTS

We thank the National Science Council, Taiwan, for supporting this study under Contracts NSC-97-2221-E-002-046-MY3 and NSC-97-2623-7-002-008-ET.

REFERENCES

(1) Osterbacka, R.; Tobjork, D. *Adv. Mater.* **2011**, *23*, 1935−1961.
(2) Kim, J. Y.; Park, S. H.; Jeong, T.; Bae, M. J.; Song, S.; Lee, J.; Han, I. T.; Jung, D.; Yu, S. *IEEE Trans. Electron Dev.* **2010**, *57* (6), 1470−1474.
(3) Chen, Z. J.; Wang, F.; Xiao, L. X.; Qu, B.; Gong, Q. H. *Sol. Energy Mater. Sol. Cells* **2010**, *94* (7), 1270−1274.
(4) Ong, K. G.; Tan, E. L.; Ng, W. N.; Shao, R.; Pereles, B. D. *Sensors (Basel)* **2007**, *7* (9), 1747−1756.
(5) Carrilho, E.; Martinez, A. W.; Whitesides, G. M. *Anal. Chem.* **2009**, *81* (16), 7091−7095.
(6) Vyas, R.; Lakafosis, V.; Rida, A.; Chaisilwattana, N.; Travis, S.; Pan, J.; Tentzeris, M. M. *IEEE Trans. Microwave Theory Tech.* **2009**, *57* (5), 1370−1382.
(7) Li, Y. F.; Ali, M. M.; Aguirre, S. D.; Xu, Y. Q.; Filipe, C. D. M.; Pelton, R. *Chem. Commun.* **2009**, *43*, 6640−6642.
(8) O'Driscoll, C. *Chem. Ind. (London)* **2009**, *19*, 9−9.
(9) Yu, J. H.; Ge, L.; Huang, J. D.; Wang, S. M.; Ge, S. G. *Lab Chip* **2011**, *11*, 1286−1291.
(10) Culbertson, C. T.; Klasner, S. A.; Price, A. K.; Hoeman, K. W.; Wilson, R. S.; Bell, K. J. *Anal. Bioanal. Chem.* **2010**, *397*, 1821−1829.
(11) Guendouz, M.; Hiraoui, M.; Lorrain, N.; Moadhen, A.; Haji, L.; Oueslati, M. *Mater. Chem. Phys.* **2011**, *128*, 151−156.
(12) Cheng, Q.; Phillips, K. S. *Anal. Bioanal. Chem.* **2007**, *387*, 1831−1840.
(13) Kall, M.; Chen, S. C., S.; Svedendahl, M.; Van Duyne, R. P. *Nano Lett.* **2011**, *11*, 1826−1830.
(14) Liz-Marzan, L. M.; Sepulveda, B.; Angelome, P. C.; Lechuga, L. M. *Nano Today* **2009**, *4*, 244−251.
(15) Oh, S. H.; Bantz, K. C.; Meyer, A. F.; Wittenberg, N. J.; Im, H.; Kurtulus, O.; Lee, S. H.; Lindquist, N. C.; Haynes, C. L. *Phys. Chem. Chem. Phys.* **2011**, *13*, 11551−11567.
(16) Yang, L. L.; Yan, B.; Premasiri, W. R.; Ziegler, L. D.; Dal Negro, L.; Reinhard, B. M. *Adv. Funct. Mater.* **2010**, *20*, 2619−2628.
(17) Lee, C. H.; Hankus, M. E.; Tian, L.; Pellegrino, P. M.; Singamaneni, S. *Anal. Chem.* **2011**, *83*, 8953−8958.
(18) Zhao, W; Ali, M. M.; Aguirre, S. D.; Brook, M. A.; Li, Y. *Anal. Chem.* **2008**, *80*, 8431−8437.
(19) White, I. M.; Yu, W. W. *Anal. Chem.* **2010**, *82*, 9626−9630.
(20) Lee, P. C.; Meisel, D. *J. Phys. Chem.* **1982**, *86* (17), 3391−3395.
(21) He, J.; Kunitake, T.; Nakao, Aiko. *Chem. Mater.* **2003**, *15*, 4401−4406.
(22) Gottesman, R.; Shukla, S.; Perkas, N.; Solovyov, L. A.; Nitzan, Y.; Gedanken. *Langmuir* **2011**, *27*, 720−726.
(23) Barr, M. C.; Rowehl, J. A.; Lunt, R. R.; Xu, J. J.; Wang, A. N.; Boyce, C. M.; Im, S. G.; Bulovic, V.; Gleason, K. K. *Adv. Mater.* **2011**, *23* (31), 3500−3505.
(24) Lamprecht, B.; Thunauer, R.; Ostermann, M.; Jakopic, G.; Leising, G. *Phys. Status Solidi A* **2005**, *202* (5), R50−R52.
(25) Xia, Q. F.; Chou, S. Y. *Appl. Phys. A: Mater. Sci. Process.* **2010**, *98*, 9−59.
(26) Tseng, S. C.; Chen, H. L.; Liu, H. W.; Yu, C. C.; Wang, L. A.; Chen, Y. P. *Phys. Chem. Chem. Phys.* **2011**, *13*, 5747−5752.
(27) Haro-Poniatowski, E.; Fort, E.; Lacharme, J. P.; Ricolleau, C. *Appl. Phys. Lett.* **2005**, *87*, 143103.
(28) Yamada, H.; Sano, T.; Nakayama, T.; Miyamoto, I. *Appl. Surf. Sci.* **2002**, *197*, 411.
(29) Kuznetsov, A. I.; Evlyukhin, A. B.; Goncalves, M. R.; Reinhardt, C.; Koroleva, A.; Arnedillo, M. L.; Kiyan, R.; Marti, O.; Chichkov, B. N. *ACS Nano* **2011**, *5*, 4843−4849.
(30) Kuznetsov, A. I.; Kiyan, R.; Chichkov, B. N. *Opt. Express* **2010**, *18*, 21198−21203.
(31) Jacobsen, D. W. *Clin. Chem.* **1998**, *44*, 1833−1843.
(32) Lawrence, N. S.; Davis, J.; Jiang, L.; Jones, T. G. J.; Davis, S. N.; Compton, R. G. *Analyst* **2000**, *125*, 661−663.